Functional connectivity uniqueness and variability? Linkages with cognitive and psychiatric problems in children

Zening Fu [1] ✉, Jingyu Liu [1,2,3,4], Mustafa S. Salman [1,5], Jing Sui [1,6] & Vince D. Calhoun [1,2,3,4,5]

Brain functional connectivity (FC) derived from functional magnetic resonance imaging has been serving as a potential 'fingerprint' for adults. However, cross-scan variation of FC can be substantial and carries biological information, especially during childhood. Here we performed a large-scale cross-sectional analysis on cross-scan FC stability and its associations with a diverse range of health measures in children. Functional network connectivity (FNC) was extracted via a hybrid independent component analysis framework on 9,071 participants and compared across four scans. We found that FNC can identify a given child from a large group with high accuracy (maximum >94%) and replicated the results across multiple scans. We then performed a linear mixed-effects model to investigate how cross-scan FNC stability was predictive of children's behaviour. Although we could not find strong relationships between FNC stability and children's behaviour, we observed significant but small associations between them (maximum $r = 0.1070$), with higher stability correlated with better cognitive performance, longer sleep duration and less psychotic expression. Via a multivariate analysis method, we captured larger effects between FNC stability and children's cognitive performance (maximum $r = 0.2932$), which further proved the relevance of FNC stability to neurocognitive development. Overall, our findings show that a child's connectivity profile is not only intrinsic but also exhibits reliable variability across scans, regardless of brain growth and development. Cross-scan connectivity stability may serve as a valuable neuroimaging feature to draw inferences on early cognitive and psychiatric behaviours in children.

Functional connectivity (FC) derived from functional magnetic resonance imaging (fMRI) data has been associated with cognition[1] and various brain disorders[2]. Brain FC is assumed to be unique to individuals previously, regardless of how the brain is engaged during scanning[3]. FC heterogeneity has long been appreciated in fMRI, even within the same population[4]. Using a multi-condition fMRI dataset from the Human Connectome Project (HCP), studies have shown that FC profile can distinguish adult participants across scan sessions

[1]Tri-Institutional Center for Translational Research in Neuroimaging and Data Science (TReNDS), Georgia State University, Georgia Institute of Technology, Emory University, Atlanta, GA, USA. [2]Department of Psychology, Georgia State University, Atlanta, GA, USA. [3]Department of Computer Science, Georgia State University, Atlanta, GA, USA. [4]Department of Neurosciences, Georgia State University, Atlanta, GA, USA. [5]School of Electrical & Computer Engineering, Georgia Institute of Technology, Atlanta, GA, USA. [6]State Key Laboratory of Cognitive Neuroscience and Learning, Beijing Normal University, Beijing, China. ✉e-mail: fzn198637@gmail.com
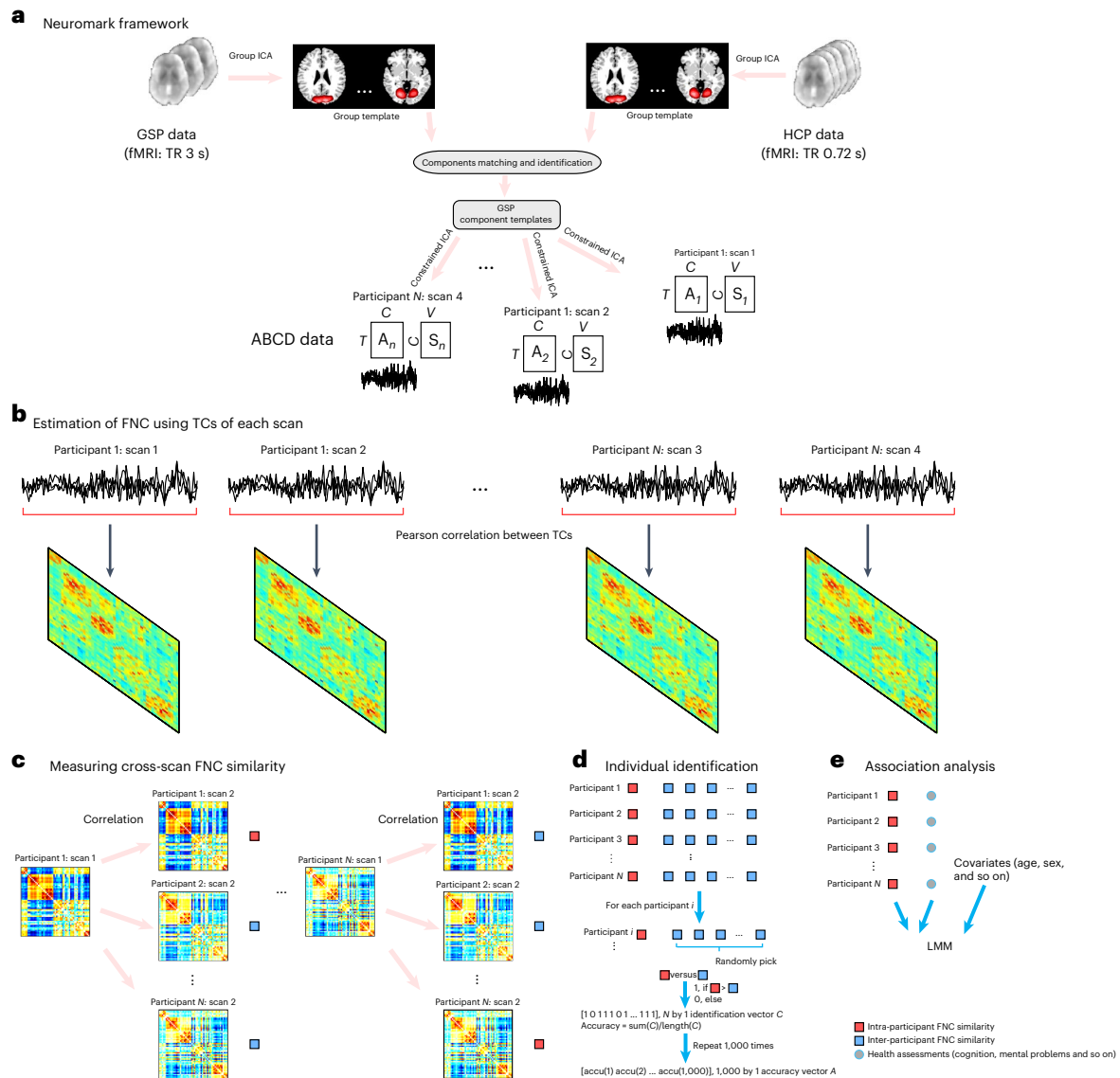
Fig. 1 | The flowchart of the FNC analysis to investigate cross-scan FNC.
a, Neuromark framework extracts robust functional components from the ABCD data. Component templates are identified using two independent data with different repetition time (TR). **b**, FNC is estimated using the TCs of components from each scan. **c**, Cross-scan FNC similarity is measured by the correlation between FNC from different scans. **d**, Individual identification is performed on the basis of the cross-scan FNC similarity. **e**, Association analysis between FNC stability (intra-participant FNC similarity) and individuals' behaviour via the LMM.

and even between distinct task conditions[5,6], acting as a 'fingerprint'. Griffa et al. proposed a structure-informed graph signal processing filtering method and applied it to a subset of HCP data to capture more unique FC to participant and cognition[5]. In another study, Horien and colleagues used four longitudinal datasets to show the uniqueness of individual FC over months to years[6]. However, brain FC is not constant but continuously changes with remarkable variations at different scales, adapting to internal and external demands[7]. That is, besides the intrinsic patterns, an individual's FC also exhibits prominent intra-participant variability, which might underlie important biological mechanisms[8]. Many existing works have only examined the FC variation within a single scan, and an individual's cross-scan FC variability has received relatively little attention from the neuroimaging field. A comprehensive understanding of cross-scan FC is necessary for developing robust FC-based biomarkers.

The human brain shows considerable growth and development during childhood[9]. Existing evidence suggests that youth might exhibit

more temporal variability in brain FC[10] compared with adults. Age is negatively associated with the variability of transient brain states identified by a clustering strategy on dynamic FC estimates[10]. The prominent variation in youths' FC can be due to more neuroplasticity in the adolescent's brain[11], though this is still far from understood. On the other hand, some other studies believed that FC is unique to an adolescent and that the FC profile can identify an adolescent from a group of participants[11,12]. In recent years, literature has provided evidence supporting the existence of both uniqueness and variability in FC[13,14]. Kaufmann and colleagues found that brain FC develops into a more stable condition, where individuals with mental health problems show a delay in the age-related stabilization of FC[13]. However, contradictive results were reported in another study, where the intra-participant FC stability was not related to age, but correlated with the development of social skills[14].

Despite such progress, we argue that the exploration of cross-scan FC has been limited, as most studies have used relatively small

Table 1 | Basic demographics of participants

Basic demographics	Baseline	Second year
Total participants	9,071	2,918
Age (month)	119.06±7.52	142.86±7.51
Sex (female/male)	4,365/4,706	1,333/1,585
Height (inch)	55.28±3.35	60.04±3.53
Weight (lbs)	82.97±23.52	107.57±31.99
Race (W/B/H/A/O)	4,771/1,325/1,863/181/929	1,631/317/629/57/284
Cognition (nihtbx_totalcomp)	86.44±8.99	89.08±10.19
Psychiatric problem (cbcl_scr_syn_totprob)	45.73±11.35	44.78±11.27
Sleep disturbance (sleepdisturb1_p)	1.72±0.81	1.99±0.86

W, White; B, Black or African American; H, Hispanic; A, Asian; O, others or unknown.

numbers of participants. The limited sample size might be a potential cause of the contradictive findings in previous studies. In addition, previous studies used samples with a wide age range, where age and brain development might introduce confounding effects in the FC similarities between scans. More importantly, most existing work has only focused on limited behaviour measures and failed to comprehensively investigate the relationships between intra-participant FC variation and a wide range of behaviour in children. The stability of FC across scans may be linked to neural mechanisms, reflected by its relevance to adolescents' neurocognitive development, adverse mental health outcomes and other healthy backgrounds. Therefore, there is a need for a reliable large-scale study to examine the FC fingerprint property, the cross-scan FC variability and their relevance to individual differences in behaviour.

In this Article, we investigate the cross-scan FC in children using a multimodal database called Adolescent Brain Cognitive Development (ABCD). The ABCD database includes more than 11,800 participants, with multiple scans collected from two longitudinal sessions. This dataset collects a comprehensive range of measures related to mental problems, cognitions and other health backgrounds[15] that are useful for the investigation of the relationship between adolescent behaviour and brain functions[16]. The novelty of our study is two-fold. First, this is a large-scale analysis of the FC fingerprint property in children. We used more than 9,000 samples from the baseline session and about 3,000 samples from the second-year session that can provide more reliable results of the fingerprint property in children. In addition, our present study used the dataset where the individuals are around the same age, which therefore is capable of precisely targeting the FC fingerprint property in pre-teen years. The second novelty of our work is that, unlike most of the FC fingerprint studies, we speculate that the cross-scan variation in individualized FC is meaningful with cognitive and psychological relevance. Recent studies have proposed several approaches to characterize the dynamic brain patterns within a single scan, which can identify individuals and predict cognitive functions, acting like fingerprinting[17,18]. While previous studies focused on the unique patterns of individualized connectome profile (static or dynamic within a single scan), our study concentrated on the intra-participant FC changes across scans, highlighting that children's FC shows substantial cross-scan variability that carries biological information associated with children's behaviour. We provided reliable evidence demonstrating that, besides the fingerprint property, individualized FC exhibits neuronally related variability across scans, which is associated with children's behaviour. We also hypothesized that FC variability in children is associated with parental psychopathology and prenatal exposure. The public health implications are that parents' conditions should be considered in relation to the variability of individualized FC in children that is associated with neurocognitive development.

Results
Flowchart of the cross-scan FC analysis
Figure 1 displays the flowchart of the cross-scan functional network connectivity (FNC) analysis. We first applied a Neuromark framework to extract robust intrinsic connectivity networks (ICNs) that are comparable across participants, scans and sessions. FNC was estimated using the time-courses (TCs) of ICNs from each scan. After obtaining the FNC matrix of each scan, cross-scan FNC similarity was measured by the correlation between FNC from different scans. The individual identification was performed based on the cross-scan FNC similarity. Finally, we investigated the associations between FNC stability (intra-participant FNC similarity) and individuals' behaviour via a linear mixed-effects model (LMM).

Functional networks
Fifty-three ICNs were extracted by the Neuromark framework, with activation peaks falling on the cortical and subcortical grey matter areas across the whole brain. The ICNs were arranged into seven functional domains according to their anatomical locations and functional information[7], including subcortical (SC), auditory (AUD), visual (VS), sensorimotor (SM), cognitive-control (CC), default-mode (DM) and cerebellar (CB) domains. Details of the spatial maps and coordinates of ICNs are provided in Supplementary Table 1 and Supplementary Fig. 2.

FNC shows high intra-participant similarity across scans
There are 9,071 participants from the baseline session and 2,918 participants from the second-year session for the within-session analysis. There are 2,290 participants with good longitudinal scans for the cross-session analysis. The basic demographics are provided in Table 1. Figure 2 displays the FNC of participants with the maximum and minimum intra-participant FNC similarity between scans. Children showed different levels of cross-scan FNC similarity. For participant 1, the FNC of scan 1 and the FNC of scan 2 were highly similar ($r = 0.9448$). In contrast, for participant 2, the FNC showed less stability between scan 1 and scan 2, where the intra-participant FNC similarity was only $r = 0.1914$. Figure 3 displays the percentage of children with an intra-participant FNC similarity higher than a given percentage of inter-participant FNC similarities, from 60% to 99%. Intra-participant FNC similarity was higher than most inter-participant FNC similarities, though intra-participant FNC variability exists. The FNC showed the highest intra-participant similarity between scan 1 and scan 2. More than 90% of participants had an intra-participant FNC similarity higher than 60% of inter-participant FNC similarities, and more than 65% of participants had an intra-participant FNC similarity higher than 99% of inter-participant FNC similarities. The intra-participant FNC showed the lowest similarity between scan 1 and scan 4. Still, more than 80% of participants had an intra-participant FNC similarity higher than 60% of inter-participant
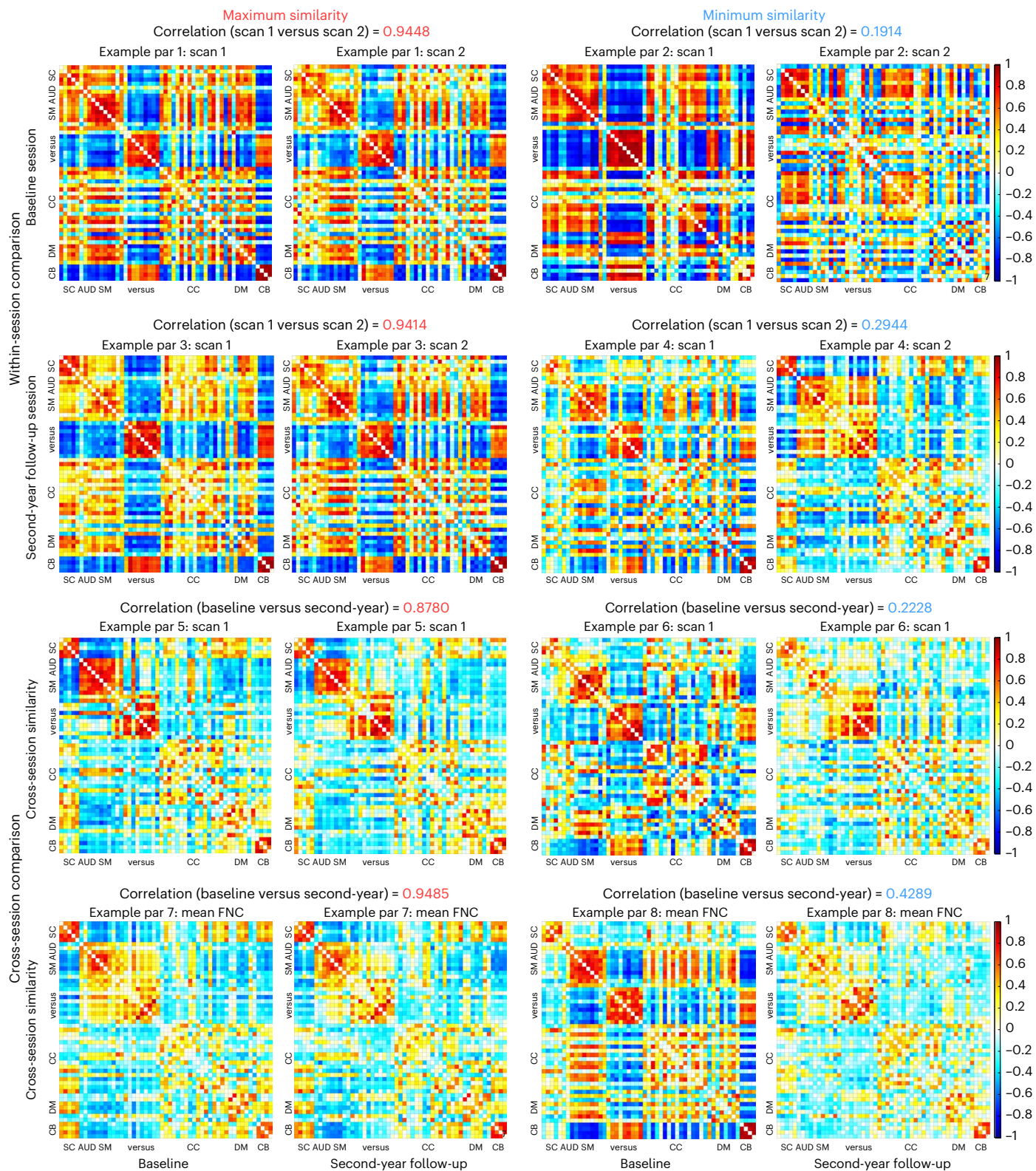
Fig. 2 | Cross-scan FNC similarity within the same session and between longitudinal sessions. FNC similarity is calculated using scans within the baseline session, within the second-year session and from longitudinal sessions (one is from the baseline and the other one is from the second year). Example participants with the maximum and minimum FNC similarity within the baseline session and the second-year session, and across longitudinal sessions. Par, participant.

FNC similarities, and about 40% of participants had an intra-participant FNC similarity higher than 99% of inter-participant FNC similarities.

These patterns are consistent when examining the scans from the second-year session. Similarly, participants showed different levels of cross-scan FNC similarity. FNC had the highest intra-participant similarity between scan 1 and scan 2 and the lowest intra-participant similarity between scan 1 and scan 4. FNC also showed intra-participant similarities between longitudinal scans. Although
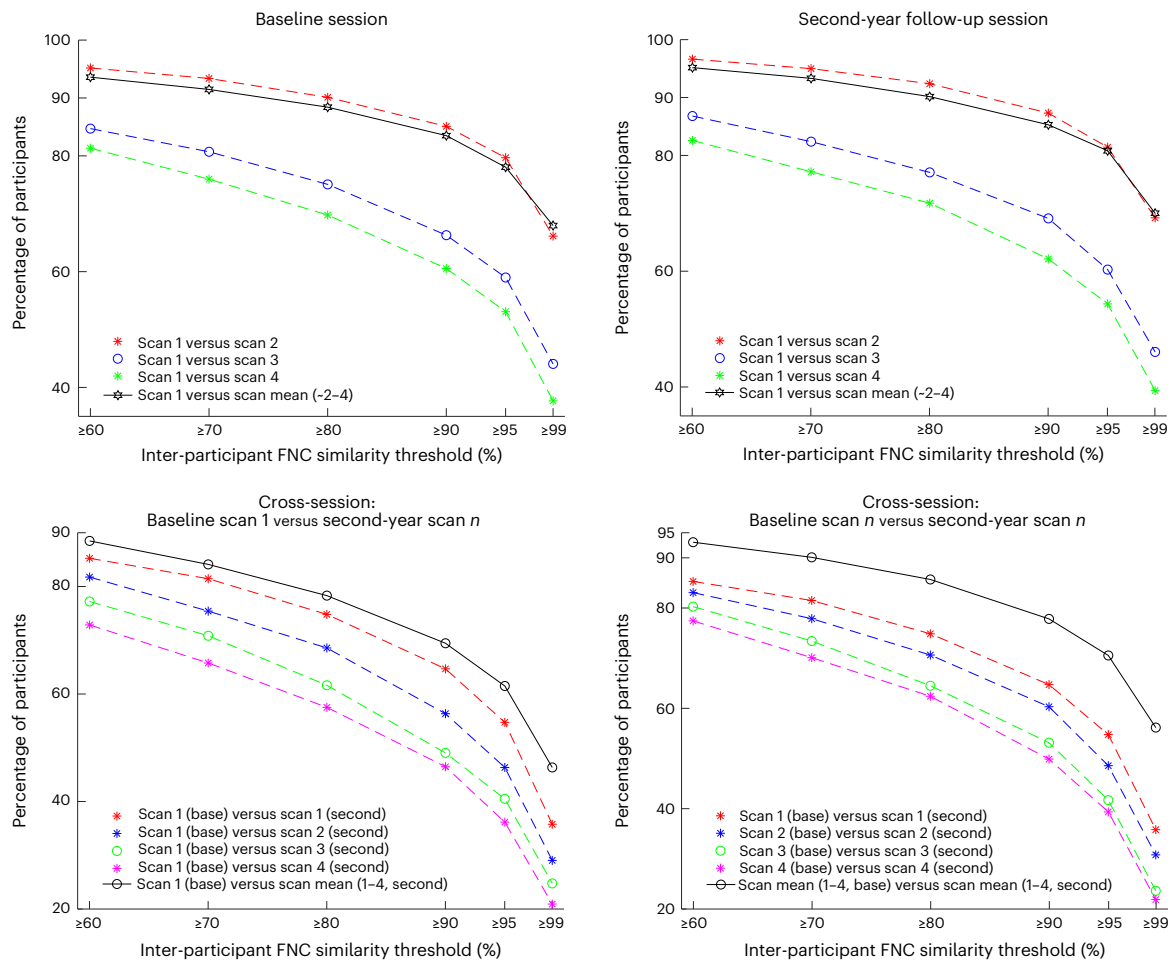
Fig. 3 | Percentage of participants with an intra-participant FNC similarity higher than a given percentage of inter-participant FNC similarities. Higher intra-participant FNC similarity is observed between scans from the same session. Intra-participant FNC similarity between longitudinal sessions is higher when FNC is averaged across scans within each session.

a 2-year time interval between scans incurred a notable decrease in the intra-participant similarity, the intra-participant similarity was still higher than most inter-participant FNC similarities, especially when the FNC was averaged within each session before measuring the similarity.

Individual identification using whole-brain FNC
Figure 4 shows the children's identification results based on the cross-scan FNC similarity. At the baseline session, the identification accuracy was 94.02 ± 0.19%, 84.81 ± 0.28%, 81.84 ± 0.30% and 93.10 ± 0.20% based on the database target of scan 1–scan 2, the database target of scan 1–scan 3, the database target of scan 1–scan 4 and the database target of scan 1–scan mean, respectively. The identification was replicated by using the second-year data. Similar to the results from the baseline, the highest identification accuracy of 95.14 ± 0.32% was achieved on the basis of the database target of scan 1–scan 2, while the lowest identification accuracy of 82.84 ± 0.51% was achieved on the basis of the database target of scan 1–scan 4. In the supplementary section 'Individual identification based on the FNC similarity between other scans', we calculated three more pairwise similarities between scans (scan 2 versus scan 4, scan 2 versus scan 4, and scan 3 versus scan 4) and performed individual identification based on these cross-scan similarities.

The individual identification was further performed using the FNC from longitudinal scans (Fig. 4b). Scans from the baseline session were the databases, and scans from the second-year session

were the targets. Despite more intra-participant FNC variations across scans, the FNC from the baseline session can still identify a child's FNC from the second-year session. The highest accuracy was 91.44 ± 0.46%, achieved by averaging the FNC across all four scans within each session before the identification. We also performed individual identification using only females or males, respectively. The overall results are in line with those obtained by pooling all participants (Fig. 4c). An interesting observation is that the longitudinal identification achieved higher accuracy in female participants, suggesting fewer brain FC changes in females around this age. It may be possible that female participants had reached a more matured brain functional state before the study, therefore resulting in fewer FC changes during the time course of the study.

The non-parametric permutation testing shows that the average identification accuracy was 50% if the identity was shuffled for each scan. The real identification accuracy was significantly higher than the accuracy obtained by the permutation tests ($P < 1.0 \times 10^{-3}$).

FNC stability correlates with cognitive performance
Besides the intrinsic patterns, individualized FNC showed notable variability across scans. Here we focused on children's cognitive performance, mental health problems, sleep conditions and screen usage. These behaviour measures have been linked to brain functions and structures in previous studies[19,20]. We could not find strong relationships between FNC stability and children's behaviour, but we observed small associations between them. The cognitive measures
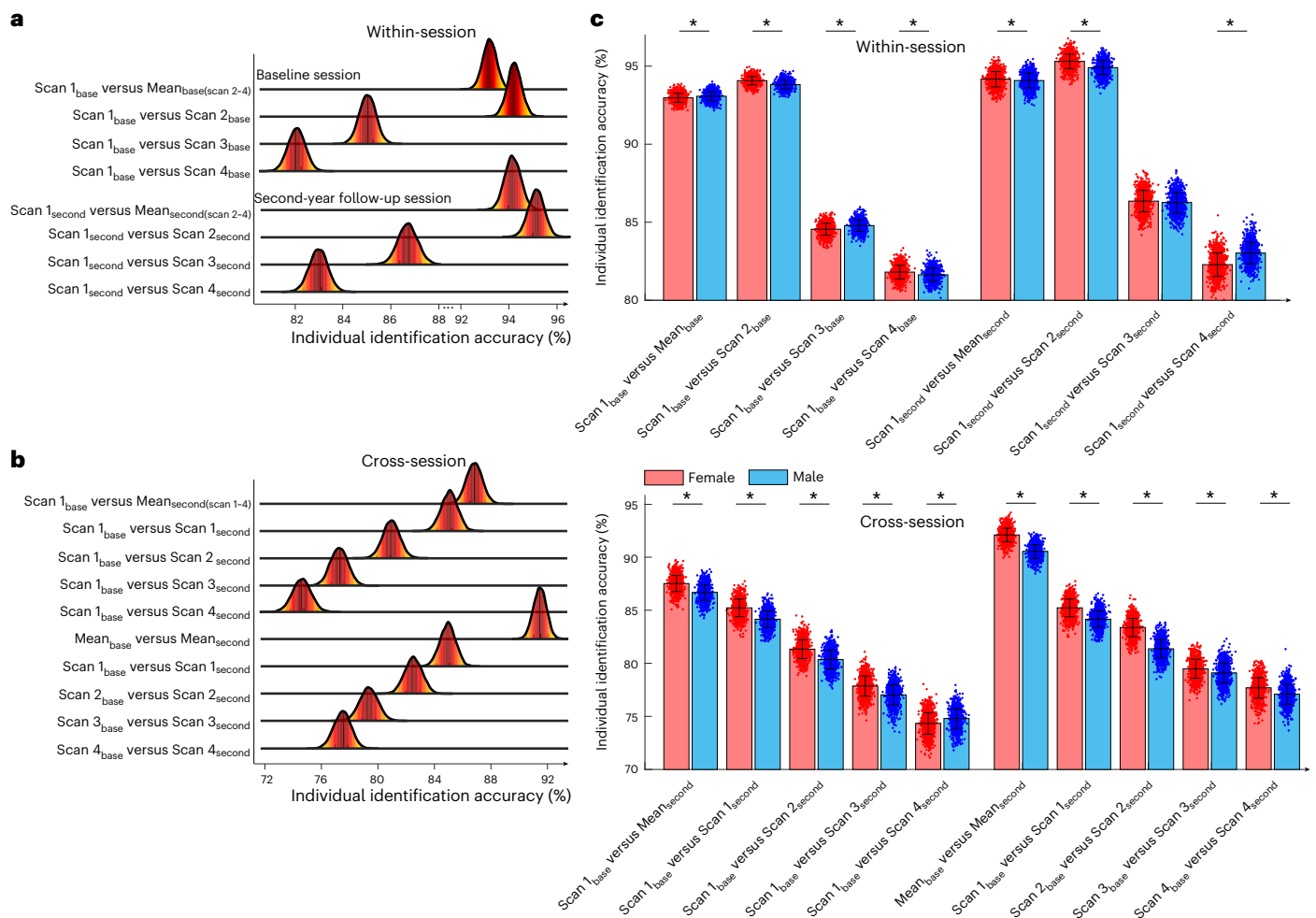
Fig. 4 | Individual identification using FNC across scans. a, Identification accuracy based on the FNC similarity between the scans within the baseline session. Scan 1 is the database, while other scans are the target. Individual identification is replicated using FNC of scans from the second-year session. **b,** Individual identification performed between scans from longitudinal sessions. Scans from the baseline session are the database and scans from the second-year session are the target. Identification accuracy drops when developmental brain changes are introduced. **c,** Individual identification is performed using only female participants or male participants. Data expressed as mean ± s.d. Each dot represents an individual identification experiment. $n = 1,000$ independent experiments for each individual identification. Averaging FNC across scans within each session can improve the performance of longitudinal identification. *Two-sample t-test, $q < 0.001$, FDR corrected.

were positively correlated with the intra-participant FNC stability (false discovery rate (FDR) corrected, $q < 0.05$; Fig. 5a). Specifically, ten out of ten cognitive summary scores were positively correlated with FNC stability, with correlation r values ranging from 0.0376 to 0.1070 (Supplementary Table 2). The Total Composite Score was the score most significantly positively correlated with the FNC stability ($r = 0.1070$, Cohen's $d = 0.2152$, $P = 4.82 \times 10^{-24}$). For the neurocognitive battery in the subdomain, the score of Toolbox Picture Vocabulary Task was the score most significantly positively correlated with the FNC stability ($r = 0.0841$, Cohen's $d = 0.1688$, $P = 1.54 \times 10^{-15}$) while the score of Toolbox Flanker Task was the score least significantly positively correlated with intra-participant FNC stability ($r = 0.0376$, Cohen's $d = 0.0753$, $P = 3.68 \times 10^{-4}$). To better visualize the correlated relationships, we divided the children into four groups from low cognitive performance to high cognitive performance according to each cognitive score (group 1: ~0–25%, group 2: ~25–50%, group 3: ~50–75% and group 4: ~75–100%) and the average cross-scan FNC stability within each group is displayed in Fig. 5b. Clear increasing trends can be observed along groups 1 to 4, indicating that children with good cognitive performance tended to have higher FNC stability.

FNC stability correlates with psychiatric problems

The psychopathological measures of children were negatively correlated with the intra-participant FNC stability. Twelve out of 20 psychiatric problem scores show significantly negative correlations with FNC stability, with r values ranging from -0.0257 to -0.0496 (FDR corrected, $q < 0.05$; Fig. 5a). The social problem score was the score most significantly negatively correlated with the FNC stability ($r = -0.0496$, Cohen's $d = -0.0992$, $P = 2.38 \times 10^{-6}$). Again, we divided the children into four groups according to each psychopathological measure. The FNC stability shows decreasing trends along groups 1 to 4, indicating that children with high psychiatric problem scores tended to have lower FNC stability (Fig. 5b).

FNC stability correlates with sleep and screen usage

We further found significant associations between FNC stability and the sleep conditions of children (Fig. 5a). Cross-scan FNC stability was negatively correlated with the sleep duration score ($r = -0.0752$, Cohen's $d = -0.1508$, $P = 7.74 \times 10^{-13}$). In the ABCD measurement system, a high sleep duration score indicates short sleep duration (1: 9–11 h; 2: 8–9 h; 3: 7–8 h; 4: 5–7 h; 5: less than 5 h). The FNC stability was also negatively correlated with the score that evaluates how long an adolescent falls
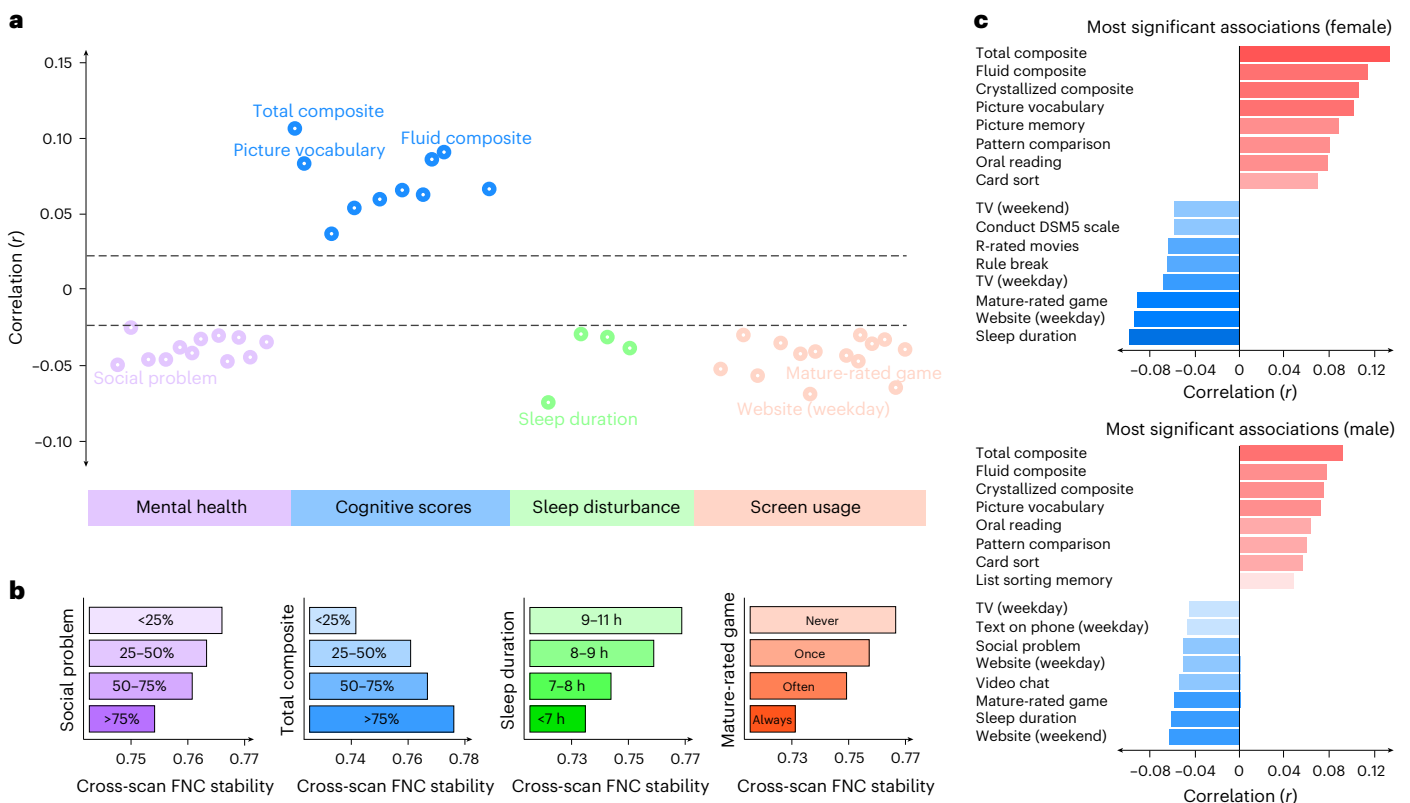
Fig. 5 | Cross-scan FNC stability is associated with children's behaviour. a, Cross-scan FNC stability is negatively correlated with mental health scores, positively correlated with cognitive performance, negatively correlated with sleep condition and negatively correlated with screen usage. The dashed lines indicate the significant correlation threshold after the multiple comparison correction (LMM correlation analysis, $q < 0.05$, FDR corrected). **b**, Children with high psychiatric problem scores tend to have lower cross-scan FNC stability. Children with good cognitive performance tend to have higher cross-scan FNC stability. Children with bad sleep conditions (for example, shorter sleep duration and longer time to fall asleep) tend to have lower cross-scan FNC stability. Children with more screen usage (for example, longer time watching TV and video) tend to have lower cross-scan FNC stability. **c**, Most significant associations between cross-scan FNC stability and children's behaviour based on only female and male participants, respectively. Results are consistent across female and male participants. Females have larger associations between FNC stability and behaviour scores.

asleep (sleepdisturb2_p). A higher score in sleepdisturb2_p indicates a longer time to fall asleep. The FNC stability was negatively correlated with other sleep behaviour of adolescents, such as sleepdisturb24_p (evaluates a child feels unable to move when waking up in the morning) and sleepdisturb26_p (evaluates a child falls asleep suddenly in inappropriate situations). Higher scores in these measurements indicate more frequently that the event happens (1: never; 2: occasionally (once or twice per month or less); 3: sometimes (once or twice per week); 4: often (three or five times per week); 5: always). The overall results indicate that children with worse sleep conditions (for example, shorter sleep duration or longer time to fall asleep) tended to have lower FNC stability (Fig. 5b and Supplementary Table 5).

Children's screen usage was also negatively correlated with cross-scan FNC stability. All 14 youth screen time utilization scores, including the use of television, internet, cell phone and video games, show negative correlations with individuals' FNC stability (FDR corrected, $q < 0.05$; Fig. 5a). Children with more screen usage tended to have lower FNC stability. Details of the correlation statistics can be found in Supplementary Table 6. The association analysis was also performed on female and male participants, respectively. Similar association patterns were observed across female and male participants, where females showed larger associations between FNC stability and behaviour scores (Fig. 5c).

FNC stability correlates with parental psychopathology

Moreover, parental dimensional psychopathology showed significant correlations with their children's FNC stability (Fig. 6a,b). Specifically, the positive questions in the parents' psychopathology assessment, including asr_q15_p (I am pretty honest), asr_q73_p (I meet my responsibilities to my family), asr_q88_p (I enjoy being with people), asr_q98_p (I like to help others), asr_q106_p (I try to be fair to others) and asr_q123_p (I am a happy person), were positively correlated with the FNC stability of children, with r values ranging from 0.0315 to 0.0583 (FDR corrected, $q < 0.05$). In contrast, the negative questions in the parents' psychopathology assessment were negatively correlated with the FNC stability of children, with r values ranging from −0.0287 to −0.0482 (FDR corrected, $q < 0.05$). These results indicate that parents with positive behaviour are associated with higher FNC stability in children while parents with negative behaviour are associated with lower FNC stability in children. We further performed a mediation analysis and found that, although children's psychopathology mediated the effect between parental psychopathology and children's FNC stability, there was a strong direct effect between parental psychopathology and children's FNC stability (Supplementary Fig. 6).

Our analysis also showed that prenatal exposure before and during pregnancy was associated with FNC stability in children. Parents with prenatal exposure to tobacco and marijuana will result in lower FNC stability in children (Fig. 6a). Also, a planned pregnancy will result in higher FNC stability in children. The age of parents during the pregnancy showed positive correlations with FNC stability as well. While older mothers will result in higher FNC stability in children, fathers aged between 30 and 40 years old (when the child was born) result in the highest FNC stability in children (Fig. 6a,b). The overall association results are consistent across females and males (Fig. 6c).
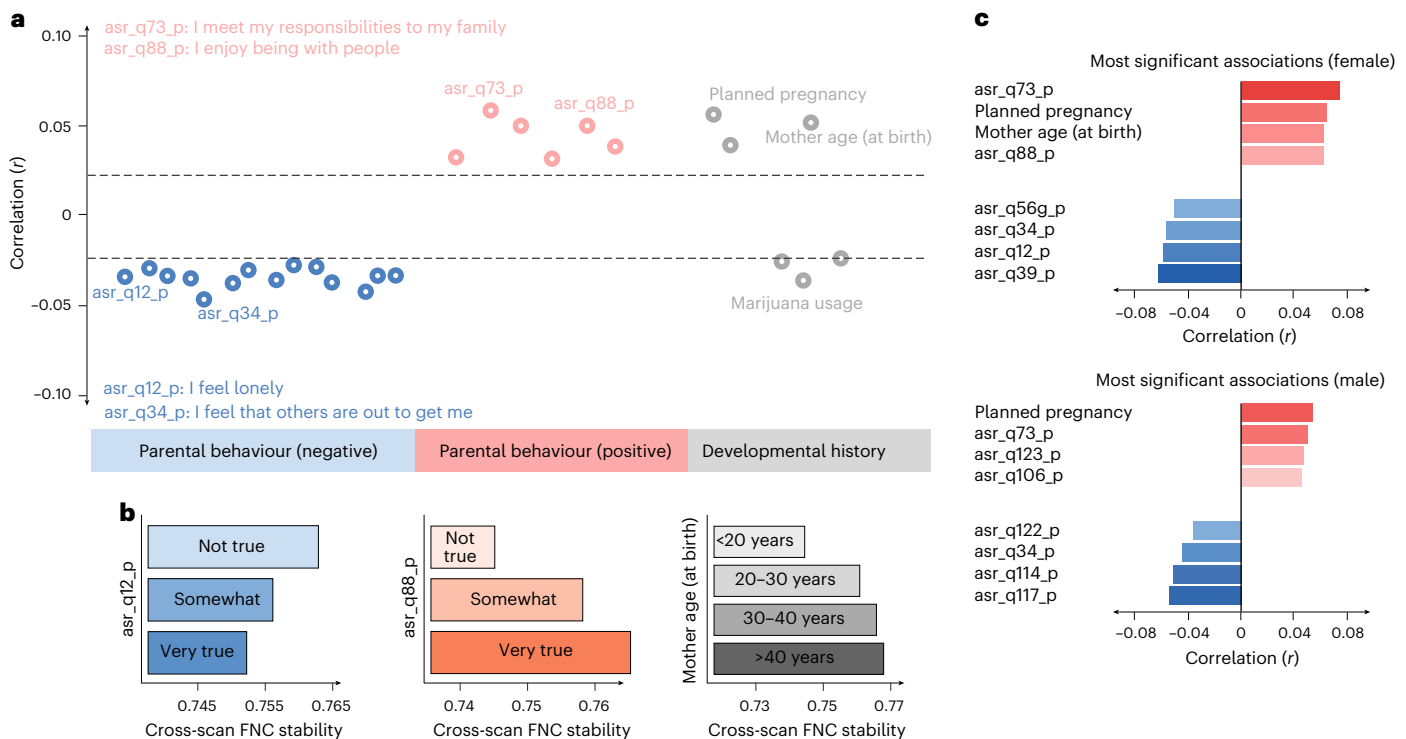
Fig. 6 | Children's FNC stability is associated with developmental history and parental dimensional psychopathology. a, Cross-scan FNC stability is negatively correlated with parental negative behaviour (for example, question q12: I feel lonely) and positively correlated with parental positive behaviour (for example, question q15: I am pretty honest). There are also significant associations between FNC stability and parents' age at birth and other developmental histories. The dashed lines indicate the significant correlation threshold after the multiple comparison correction (LMM correlation analysis, $q < 0.05$, FDR corrected). **b,** Children with parents having negative psychopathology tend to have lower cross-scan FNC stability. Children with parents having positive behaviour tend to have higher cross-scan FNC stability. The parents' age is positively correlated with children's FNC stability. **c,** Most significant associations between cross-scan FNC stability and developmental history and parental psychopathology based on only female and male participants, respectively. Results are consistent across female and male participants.

FNC stability predicts children's cognition

To show that multivariate predictive techniques can capture larger effects between FNC stability and children's behaviour, we implemented a partial least squares regression (PLSR) for predicting children's cognition. We chose the domain-based cross-scan FNC stability as the imaging feature and selected the total composite cognitive score as the target measure. The results of the PLSR show that combining 26 domain-based cross-scan FNC stability can predict the total composite score ($r = 0.1570 \pm 0.0013$, $P < 1.0 \times 10^{-3}$). We found that the effect size ($r = 0.1570$) is larger than the effect size from the univariate analyses ($r = 0.1070$). We also implemented the same predictive model to the other two composite scores (Crystallized Intelligence Composite and Fluid Intelligence Composite), and the results are highly consistent, where multivariate models provide larger effect sizes in the association analysis ($r = 0.1344$ and $r = 0.1306$, compared with $r = 0.0911$ and $r = 0.0865$ by univariate analyses).

We further introduced a method to evaluate cross-scan FNC stability for each pair of FNC, which can provide high-dimensional FNC stability features for building the prediction model. Detailed methodologies are provided in the section 'Multivariate model to predict children's behaviour' in Supplementary Information. Our results show that combining pairwise FNC stability features with PLSR can predict the total composite score with a much larger effect size ($r = 0.2855 \pm 0.0020$, $P < 1.0 \times 10^{-3}$, permutation test, Supplementary Fig. 7). We also implemented the same model to predict the other two composite scores, and the results were highly similar, where multivariate models based on the pairwise FNC stability provided much larger effect sizes in the association analysis ($r = 0.2932 \pm 0.0016$ and

$r = 0.2129 \pm 0.0030$, $P < 1.0 \times 10^{-3}$, permutation test, Supplementary Fig. 7). More interestingly, when applying the cognition-predictive model (based on Crystallized Intelligence Composite) defined in the baseline data to second-year data, we observed a significant correlation between actual and predicted cognitive scores controlling for the covariates ($r = 0.2689$, $P = 1.0 \times 10^{-26}$).

Discussion

Our work attempts to investigate the FC fingerprint and variability in children at a large scale. We found that children's FC shows intrinsic patterns and variations across scans. On the one hand, the individualized FC patterns allow the identification of individuals among a pool of children. On the other hand, the variations of individualized FC across scans are substantial and convey psychological and physiological information underlying distinct behavioural phenotypes in children. Although the univariate brain–behaviour associations are significant but small, we proved that multivariate methods could help to capture much larger effects between FNC stability and children's behaviour. Given this foundation, future neuroimaging studies should focus not only on the FC fingerprint property but also on the intra-participant FC variability, which might provide a different window into neuropsychological mechanisms.

Fingerprint property of children's FNC

Brain FC and its network analogue, FNC, are believed to provide a window into brain function and intrinsic brain organization[21]. Adults' FC profile shows substantial inter-participant variability, and such variability can distinguish individuals from another scan[3]. Unlike

adults, children show more intra-participant variability in FC due to the developments and maturation in the brain[22]. Heterogeneous brain states and confounding effects in youths (for example, head motions)[23] might also influence individual identification. In the section 'Individual identification and head motions' in Supplementary Information, we found that the head motion parameters (rotations and translations) can distinguish individuals between scans (slightly higher than the accuracy obtained by the permutation tests). Therefore, we performed additional analyses to demonstrate that our processing has successfully removed much of the motion artefact, and the FNC fingerprint property in children is not mainly driven by the similar head motions of the data.

Although some previous studies suggested that the youths' identification is not different from the adults'[11] and the stability of paediatric FC is not correlated with age[14], a contradictory finding by Kaufmann et al. showed that inter-participant FC distinctiveness increases with age[13]. The opposite findings from these studies might be due to the small sample size used for the investigation, which is easily biased by the sampling variability[24]. Via a large-scale analysis of more than 9,000 children, we observed robust cross-scan FNC similarity in children, which slightly increased in the second-year session. Interestingly, the identification accuracy decreased (the intra-participant FNC variability increased) as the time interval of scans increased. Our result provides evidence that FC exhibits cross-scan variability at an early age, and the assumption of FNC uniqueness might oversimplify the interrelationships between brain regions. The different occurrences of dynamic states could be one potential cause driving the FNC less similar as the time interval increased. The brain state in fMRI is a conceptual analogy to electroencephalogram (EEG) microstates, which is one of the most popular notions widely used to explore transient brain patterns during the resting state[7,25]. Existing evidence has demonstrated that some brain states show continuously increasing or decreasing occurrences during the scan[7,26,27]. Using simultaneous EEG–fMRI, our previous work found that a dynamic state with thalamocortical anticorrelation is associated with reduced EEG α power and increased δ and θ power, showing increasing occurrence over time, possibly reflecting the decreased vigilance[27]. We speculate that as participants stay in the scanner for a longer time, the brain changes its occurrences in different dynamic states that might influence the overall FNC patterns, potentially resulting in less similarity to the initial 'resting-state' FNC.

We successfully performed the individual identification between longitudinal scans with a 2-year interval, although with reduced overall accuracy. This finding is in line with a previous result based on a relatively small sample size, which suggested that a larger time interval can incur a notable decrease in identification accuracy[11]. We further found that averaging FNC across scans within each session can increase accuracy. Growth and development inside the children's brain will introduce FC variation intra-participant, associated with children's neurodevelopment and behaviour[28]. Averaging FNC within the same session can mitigate the heterogeneity induced by transient brain states but not the variability induced by brain development. Our result suggests that the decreased identification accuracy between longitudinal scans can be due to both brain development and the difference in the temporal brain conditions. The successful longitudinal identification further supports that the FC profile contains fundamental properties unique to each child, regardless of the FC developments during adolescence[11]. Another interesting finding of the FNC fingerprint property is that cross-session identification achieves higher accuracy in female participants. This finding suggests that females at the age of 9–11 years show fewer age-related FNC changes. Sex differences in developmental trajectories have been widely reported in the literature, and the investigation of sex-related developmental trajectories might help to clarify the allometric issues previously discussed[29]. An EEG resting-state study has also found sex differences in microstate occurrences from childhood to adolescence[30]. Specifically, there is a particular development trajectory of increased duration of the microstate in males, but not in females.

Another work based on a subset of the data from the Child Psychiatry Branch at the National Institute of Mental Health demonstrated that, while females have their cerebral volume peaking at age 10.5 years, males have their volume continuously growing until 14.5 years old[31]. Our result is in line with these previous findings and provides further evidence of the sex differences in functional brain development from childhood to adolescence. While females' FNC becomes stable at the age of 9–11 years, males' FNC shows more variability at this age. We speculate that such a late maturation of FNC in males might be linked to the risk for abnormal neurodevelopmental processes that could facilitate the onset of schizophrenia[32].

FNC stability and children's behaviour
Although the brain–behaviour associations are small, the balance between cross-scan FNC similarity and variability does not appear to be driven by random noise. Cross-scan FNC stability was positively correlated with cognitive performance, including reading recognition, pattern comparison, memory and so on. Previously, neuroimaging studies focused on FC strength and suggested that it is relevant to individual differences in behaviour. However, brain FC shows considerable variation between tasks and rest, across scans, and even within a single scan[8,27,33]. Spontaneous FC variations can predict the performance of different cognitive tasks[34]. Literature also showed that individuals with temporally stable FC show advanced cognitive performance, reflected by increased accuracy and more stable response time[35,36]. Our finding has extended the investigation of FC variability within a single scan to the investigation of FC stability across scans and showed robust relationships between cross-scan FC stability and cognitions. A possible explanation of this finding is that the resting state is in a 'relaxed' brain condition that ameliorates the adaptive reconfiguration of brain networks in the context of cognitive tasks. A stable FC during the execution of cognitive tasks is associated with successful cognition and difficult task conditions require increased stability of FC[35,36]. The stable FC during the resting state might facilitate the brain switching from a relaxed condition to a task-demand condition that purportedly requires sustained cognition, consequently resulting in better cognitive performance[37].

In addition to the associations with cognitions, we found negative correlations between FNC stability and children's mental health. Children with less cross-scan FNC stability have more dimensional psychopathological problems and more frequent symptoms of mania. This result is in line with a previous finding showing that the stability of FC is related to psychiatric disorders[13]. Although they did not identify different FC distinctiveness between groups in children (<14 years), they found that adolescents with increased psychiatric symptom scores show less FC distinctiveness compared with controls[13]. Our result extends their finding by showing that the associations between FC stability and dimensional psychopathology exist during a very early age (~9–11 years). One interpretation of these associations is that decreased FC stability underlies the dysregulated brain rhythms that characterize psychiatric problems. Of note, increased rumination is associated with higher medial prefrontal cortex to insula FC variability, suggesting that the intra-participant FC heterogeneity might trigger rumination by enhancing sensitivity to self-referential information[38]. It is also suggested that the unstable FC may be associated with deficits in executive functioning and reflect weaknesses in brain circuits responsible for cognitive control[39]. The strongest correlation between FC stability and children's mental health was found with the social problem score in our study, which is an essential replication of the finding by Vanderwal et al.[14]. Using children and adolescent samples with ages ranging from ~6 to 21 years, they found that lower FC stability is associated with a higher social responsiveness scale, a popular measure of social skill problems. These cross-study results indicate a surprisingly tight coupling between FC stability and social skills. A growing body of literature has linked dynamic FC patterns to psychiatric problems. Individuals with

autism spectrum disorder have larger FC variability in time, associated with the increase depending on autism symptom severity[40]. Using magnetoencephalography, researchers have shown that patients with schizophrenia exhibit more trial-to-trial network topology variability during a two-back working memory task[41]. Increased FC variability has also been observed in both patients with depressed bipolar disorder and major depressive disorder, who shared overlapping symptoms that typically confound the diagnosis[42]. Our results complement the prior work by showing that an individual's FNC exhibits reliable variability across scans, which might signify underlying biological mechanisms in mental health. The stability of cross-scan FNC can add information to the connectivity strength and will be a potential brain feature that predicts early psychiatric problems in children.

Our analysis further showed that the FNC stability of children is also associated with parental conditions. The development history of children can be an important indicator of later mental and psychical behaviour in youths[15]. Prenatal cannabis exposure is associated with a greater risk for psychopathology in adolescents[43]. Our present study found that prenatal tobacco and marijuana exposure is associated with lower cross-scan FNC stability during middle childhood. Considering the associations between FNC stability and cognition and dimensional psychopathology, this result underscores the potential to use FNC stability to advance our understanding of the relationships between prenatal drug usage, cognitive developments and mental health among offspring. Another interesting finding of our present study is that parental psychopathology was correlated with the FNC stability of children, where higher FNC stability in children was associated with more positive behaviour and less negative behaviour in their parents. We speculate that the family environment might influence the stability of FC in children. This speculation is supported by a further analysis showing a positive correlation between children's FNC stability and neighbourhood safety, an important living environmental factor. The inherited characteristic can be another cause of these relationships. Analysis including genetic data is needed in future studies for validating this hypothesis.

The smaller-than-expected associations between FNC stability and behaviour drive us to perform additional multivariate analyses to show the neurocognitive relevance of FNC stability. We implement a PLSR method combined with FNC stability to successfully predict the children's cognition with much larger effect sizes. We also demonstrated that the behaviour-predict model constructed on the basis of the baseline data could predict children's cognitive performance in the second-year session, which further suggests the robust linkages between FNC stability and children's cognition. Overall, the multivariate results prove that FNC stability is a reliable neuroimaging feature that can be combined with multivariate analyses to detect reliable effects on children's behaviour.

Limitations and future directions

We noted that, across all univariate association analyses between FNC stability and children's phenotype variables, the highest correlation was $r = 0.1070$ ($d = 0.2152$). Cohen suggested $d = 0.2$ as a lower threshold for 'small' effect size. However, this threshold is based on the beta error that Cohen estimated as four times the alpha error, which is somehow arbitrary and should not be interpreted rigidly[44]. Effects in psychological research are much smaller than they appear from past publications, implying that Cohen's magnitude might not be appropriate because it is guided by the typical effects that have been found in the past in a specific area of research[45]. A recent publication in psychological science has highlighted the dangers of a publication culture that continues to demand large effects that can be probably inflated and ignored small effects that are most likely to be true[46].

Imaging features have been widely linked to the variation in cognitive ability and psychopathology using univariate methods, typically with relatively larger associations ($r = \sim 0.2$–0.8) reported

in small-sample neuroimaging studies. However, brain–phenotype association findings usually suffer high levels of replication failures. Among many factors that might contribute to the poor reproducibility of the previous results, the small sample used in the studies is the most challenging. Based on the analyses of the largest databases in the neuroscience field (ABCD, UK Biobank and HCP), a recent study demonstrated that the real brain–phenotype associations are much smaller (linear correlation $r < 0.1$) than previously assumed, and the precise characterization of brain–phenotype associations requires large samples[24]. More importantly, the statistical errors were pervasive across sample sizes. The false negative rates were very high (~75–100%) even for samples as large as 1,000, where half of the significant relationships were inflated by at least 100% (ref. 24). That is to say, most previous MRI studies focusing on the brain–phenotype associations might not be sufficiently powered to find reasonable effect sizes, and the reported large associations might be solely due to effects inflated by chance[24].

Such small brain–phenotype associations might be due to the heterogeneity of the general population or the imprecision of phenotyping in big data. A recent study has shown that the reliability of neuropsychological scores has significant effects on characterizing the associations between biology and psychopathology[47]. For example, sampling biases, inconsistent phenotyping and phenotypic complexity can have great impacts on the reliability of phenotypic scores, which further influences the precise characterization of relationships between brain imaging features and human behaviour. In future studies, we can apply strategies for enhancing the precision of phenotyping, such as increasing phenotypic resolution by using the measures that have already been optimized within an item response theory framework, which is a sophisticated approach to phenotypic scale construction and refinement[48].

We also performed the association analyses between FNC uniqueness and children's cognitive performance and mental health, where the results are put in the section 'Associations between FNC and cognition/mental health' in Supplementary Information. Our results (Supplementary Figs. 8 and 9) show that the associations between FNC and behaviour have small effect sizes similar to those between intra-participant FNC variability and behaviour. Although the correlations between FNC uniqueness and behaviour might be less reproducible between sessions and the existence of intra-participant FC variability might raise the question about the reliability of resting-state FC, we do not intend to argue that resting-state FNC is an unreliable indicator of phenotypic cognitive and mental health variables. The human brain is a highly dynamic system that constantly integrates and coordinates different neural populations, where FC is not constant but shows substantial variability in the temporal scale[7,27,49]. But it should be noted that our present work also found that different FC exhibit different levels of variations across scans. This suggests that some resting-state FC might show strong reliability across trials while others exhibit more variations. FC fingerprint property and FC variability might provide complementary information to each other, and the investigation of both features might advance the association and prediction analysis in biomarker research. It could be possible that, for predicting some phenotypes, using either feature alone might be better, while for predicting other behaviour scores, combining both can improve the performance[50]. Future neuroimaging studies might also provide more moment-by-moment monitoring during the scan, which will help to guarantee the participants are in similar conditions during the scanning, probably beneficial for more precise characterization of brain signatures associated with complex human behaviour.

Methods
Participants and image acquisition
The present study used a longitudinal dataset shared by the ABCD, the largest long-term study of brain development and child health in

the United States (https://abcdstudy.org/). We used release 3.0 of the ABCD dataset, containing over 11,800 children aged 9–10 years (at baseline), with two imaging sessions (baseline and the second-year follow-up) and multiple resting-state scans within each session. Our study is under Application ID 13591, and we downloaded the ABCD FastTrack images with recommended active series from NDA. The ABCD study incorporated a comprehensive range of measures, including neurocognitive battery, physical and mental health assessments, and other health backgrounds, to assess predictors and outcomes related to different domains[15,16]. The parent's full written informed consent and the child's assent were obtained under protocols approved by the institutional review board (IRB). The University of California, San Diego provided centralized IRB approval, and each participating site received local IRB approval.

We pre-processed the raw resting-state fMRI data using a combination of the FMRIB Software Library (FSL) v6.0 toolbox and Statistical Parametric Mapping (SPM) 12 toolbox, under the MATLAB 2020b environment. The pre-processing steps included: (1) rigid body motion correction; (2) distortion correction; (3) removal of dummy scans; (4) normalization to standard Montreal Neurological Institute space; and (5) smoothing with 6 mm a Gaussian kernel. We performed data quality control on the pre-processed fMRI data via the Neuromark framework[51]. For the within-session analysis, there are 9,071 participants with four good scans from the baseline session and 2,918 participants with four good scans from the second-year session. For the cross-session analysis, there are 2,290 participants with four good scans from the baseline session and also four good scans from the second-year session. The basic demographics can be found in Table 1. Details of the fMRI pre-processing and quality control can be found in the section 'Quality control' in Supplementary Information.

Neuromark framework

To capture reliable ICNs and their corresponding TCs for each participant and each scan, a robust independent component analysis (ICA)-based framework called Neuromark[51] was applied to the ABCD data. Unlike atlas-based methods that typically assume fixed brain regions across participants, Neuromark can identify brain networks comparable across participants and scans, adapting to single-scan variability with the networks. It can retain more single-scan variability in the estimation of network-related features, which better fits our current study aim. The effectiveness of Neuromark has been demonstrated in previous work, with a wide range of brain markers and abnormalities identified in different populations[25,52–56].

Two healthy controls datasets, the HCP (823 participants after the participant selection) and the Genomics Superstruct Project (GSP; 1,005 participants after the participant selection), were used for the construction of the network templates. These two datasets have different temporal resolutions and were pre-processed via different pipelines. We chose them because we want to capture robust network templates that are reproducible across different scenarios. High model order (order 100) group ICA was performed on each dataset, and then the independent components (ICs) from the two datasets were matched by examining the similarity of their spatial maps[57]. Those pairs were considered consistent and reproducible across the GSP and HCP datasets if their spatial correlation was ≥0.4. A correlation value ≥0.25 has been shown to represent a significant correspondence ($P < 0.005$, corrected) between components, and here we used a higher threshold because we would like to identify more reliable and consistent ICs. The matched IC pairs were labelled as ICN templates or noise components by inspecting the locations of the peak activations of their spatial maps and the low-frequency fluctuations of their TCs. The reproducible templates were used as the spatial network priors to back-reconstruct spatial maps and TCs for the ABCD data. Specifically, we used the multivariate-objective optimization ICA with reference[58] to estimate single-scan spatial maps

and TCs. This method used a multiple-objective function optimization algorithm, taking only the network templates and the scan-specific fMRI data as the inputs. There are two objective functions, one is to optimize the independence of networks in the single-scan fMRI data, and the other one is to optimize the similarity between the scan-specific networks and the network templates. To combine these two objective functions, a linear weighted sum method was applied[51]. After the optimization, single-scan networks were obtained, which not only show scan-specific network patterns but also are comparable across scans and participants. Note that principal component analysis (PCA) was performed before single-participant ICA back-reconstruction. In PCA, the global mean signal per timepoint was removed as the standard PCA processing step during participant-level PCA reduction. This technical point is detailed and explained in ref. 27. Therefore, the global signal has been removed in the PCA step in the Neuromark framework, which will not influence the estimation of FNC between TCs. More details of the Neuromark framework are provided in ref. 51.

FNC

We performed four additional post-processing steps to carefully regress out the remaining noise in the TCs of ICNs: (1) detrending linear, quadratic and cubic trends, (2) removal of detected outliers, (3) multiple regression of the head motions parameters (three rotations and three translations) and their derivatives, and (4) band-pass filtering with a cut-off frequency of 0.01–0.15 Hz. Pearson correlation coefficients between post-processed TCs were calculated to measure the FNC for each scan.

FNC similarity and participant identification

We calculated the correlation between whole-brain FNC from different scans to measure the FNC similarity. The correlation was calculated between the FNC of scan 1 and the FNC of the other scans, resulting in four comparisons (scan 1 versus scan 2, scan 1 versus scan 3, scan 1 versus scan 4, and scan 1 versus mean (FNC) across ~2–4). For each comparison, the correlation between the FNC of scans from the same participant was the intra-participant FNC similarity (stability) and the correlation between the FNC of scans from different participants was the inter-participant FNC similarity. Therefore, for each participant (in each comparison), there were one intra-participant similarity and 9,070 inter-participant similarities. Then we calculated the percentage of children having an intra-participant FNC similarity higher than a given percentage of inter-participant FNC similarities (60%, 70%, 80%, 90%, 95% and 99%).

We performed individual identification using the FNC similarity from each comparison. For each participant, we compared their intra-participant FNC similarity with a randomly picked inter-participant FNC similarity. The predicted identity was that with the larger correlation value. We performed this step for every participant to obtain an identification vector, which can be used to calculate the overall identification accuracy. The whole procedure was repeated 1,000 times to estimate the distribution of the identification accuracy. We implemented non-parametric permutation testing to assess the statistical significance of identification accuracy. We permuted participant identity for the FNC of scans to shuffle the intra-participant and inter-participant FNC similarity. The same identification was performed 1,000 times on the permuted data to have the identification accuracy for the permuted data. The individual identification was further performed using only females or males to examine the sex-related difference.

We also calculated the correlations between other scans (scan 2 versus scan 4, scan 2 versus scan 4, and scan 3 versus scan 4) and performed individual identification based on these cross-scan similarities. The identification was further performed using domain-based FNC to investigate more domain-specific fingerprint properties.

Second-year data and longitudinal identification

To show that the within-session FNC similarity is robust to age, we calculated the FNC similarity between scans from the second-year session. The same identification was performed using the FNC similarity between scans. To investigate whether the FNC profile can identify an individual from a longitudinal scan while there are developmental changes in the brain, we further measured the FNC similarity between scans from the baseline session and scans from the second-year session and then performed the identification based on the FNC similarity between longitudinal scans.

Cognitive measures

The cross-scan FNC stability was measured by the intra-participant similarity between the FNC of scan 1 and mean FNC across scans ~2–4 using the baseline data. To show the test–retest reliability of the associations, we also replicated the results)1) using FNC stability evaluated by different intra-participant similarity measures, (2) controlling for head motion in the LMM, (3) using participants with small head motions, (4) using participants collected by the same scanner and (5) using the second-year data.

We first investigate the associations between FNC stability and cognitive assessments. Note that, although there are multiple resting-state scans at the baseline and the second-year sessions, for each assessment of each participant, there is only one value for the baseline session and one value for the second-year session. The cognitive performance of each adolescent was measured via the NIH Cognition Battery Toolbox (abcd_tbss01)[16]. Higher scores indicate better cognitive performance. The NIH neurocognitive battery contains seven distributional characteristics, including the Toolbox Picture Vocabulary Task, the Toolbox Oral Reading Recognition Task (TORRT), the Toolbox Pattern Comparison Processing Speed Test (TPCPST), the Toolbox List Sorting Working Memory Test (TLSWMT), the Toolbox Picture Sequence Memory Test (TPSMT), the Toolbox Flanker Task and the Toolbox Dimensional Change Card Sort Task (TDCCS). There are also three composite scores, including a Crystallized Intelligence Composite and a Fluid Intelligence Composite, and a Total Score Composite. In total, ten cognitive scores were used in the analysis. Detailed information on each score can be found in ref. 16.

Mental health measures

The associations between cross-scan FNC stability and children's mental health conditions were also investigated. The mental health conditions of children were measured by the Parent-Child Behavior Checklist Scores (CBCL, abcd_cbcls01). These checklist scores contain 11 syndrome scales related to psychiatric problems and 1 total Syndrome Scale, 6 DSM-Oriented scales and 3 CBCL Scale2007 Scales. In total, 20 scores from the CBCL Scores were used for the investigation. The ABCD Parent General Behavior Inventory-Mania (abcd_pgbi01) was also used to assess the subsyndromal mania. It contains ten scores that evaluate the children's behaviour of mania. Higher scores on mental health measures indicate dimensional psychopathology.

Sleep conditions and screen usage

The assessments of sleep conditions and sleep disorders of children were measured by ABCD Parent Sleep Disturbance Scale for Children (abcd_sds01). It includes 26 questionnaires to evaluate the sleep disturbance of each child. For example, question 1 is 'How many hours of sleep does your child get on most nights?' and question 2 is 'How long after going to bed does your child usually fall asleep?'. The scores will be between 1 and 5, with a higher score indicating a worse sleep condition (for example, fewer hours of sleep and longer time to fall asleep). The screen time utilization of youth, which is measured by the ABCD Youth Screen Time Survey (abcd_stq01), was also used to investigate its relationships with cross-scan FNC stability. It contains 14 scores that evaluate the screen usage of a child during the weekdays and weekends, with higher scores indicating longer screen usage.

Parental behaviour and prenatal exposure

We were also interested in the potential relationships between parental factors and children's FNC stability. The prenatal exposure before and during pregnancy, measured by ABCD Developmental History Questionnaire (dhx01), was used for the investigation. We focused on prenatal exposure to tobacco, alcohol and marijuana, and the parents' age when the child was born. The parental dimensional psychopathology, measured by ABCD Parent Adult Self Report Raw Scores Aseba (pasr01), was also used in the analysis. These scores evaluate parental psychopathology from either a positive question (for example, question q15: I am pretty honest) or a negative question (for example, question q12: I feel lonely). The higher scores in the positive question indicate a better condition of parents while the higher scores in the negative question indicate a worse dimensional psychopathological condition.

Association between cross-scan FNC stability and behaviour

Assuming moderate observational errors (~5% of the mean) in resting-state fMRI data and only a weak effect on the brain–behaviour associations[24] (~10% of the variability in X explained by Y), the requested sample size to achieve power equal to 0.80 and a type I error equal to 0.05 in the correlation analysis is 783. Our sample size is much larger than this number, which proves that we have sufficient samples to conduct brain–behaviour association analyses. An LMM was implemented to investigate the associations between cross-scan FNC stability and behavioural assessments. The LMM was also used to examine the associations between children's FNC stability and their parents' conditions and neighbourhood safety. The ABCD data contain related data at sites and within families due to twins and siblings. The LMM can model families nested within the site to take account of this effect. It has been successfully applied in previous ABCD studies and identified meaningful brain–behaviour associations with a wide range of individual behaviour[19,59]. In this work, cross-scan FNC stability was modelled as the dependent variable, while each score/behaviour was modelled as a fixed effect. Age, sex, race, height and weight were modelled as other fixed effects. We used the sex of the participant at birth, which is the assignment as male or female based on the biological attribute. Birth sex is measured by the PhenX toolkit. The family structures and sites were modelled as random effects[19]. The correlation r value, t-statistic and effect size Cohen's d were obtained for each association analysis to reflect the relationship between FNC stability and a behavioural score. The results were corrected by FDR correction[60] across children's behaviour measures.

The LMM analysis was also performed using only female participants and male participants, where age, race, height and weight were modelled as fixed effects, and the family structures and sites were modelled as random effects.

Multivariate model to predict children's behaviour

Here we implemented a multivariate predictive technique, namely PLSR, to predict children's behaviour. We aimed to show that FNC stability is a reliable feature that can be combined with the multivariate method to detect larger effect sizes of associations with behaviour variables. We used the domain-based cross-scan FNC stability and the pairwise FNC stability as the imaging feature and selected the composite cognitive score as the target measure. We utilized 10-fold nested cross-validation with 1,000 random replications to avoid circularity bias. The predictive model was then applied to the testing data, generating a predictive score for each participant in the testing data. By iteratively designating each fold of data as a testing set once, we can obtain the predictive scores for all participants. Model performance was quantified as the correlation r between actual and predicted scores averaged across 1,000 repetitions. The same covariates were controlled in cross-validation to show that our predictive models are robust to these confounds. To examine the significance of the correlation, we performed a non-parametric permutation test by shuffling

the correspondence between imaging features and the target measure 1,000 times and then repeating the nested cross-validated predictive analysis, generating a null distribution of 1,000 correlations. Then, the significance of the correlation was estimated by calculating the frequency with which the permutation-derived correlations exceeded the actual correlation.

We further investigated whether the behaviour-predict model constructed using the FNC stability from the baseline data can predict children's behaviour in the longitudinal sessions. PLSR was first utilized to define a cognition-predictive model using the pairwise FNC stability from the baseline data. Next, the weight map from the constructed model was obtained by extracting the regression coefficient for each feature. Then, the dot product of vectorized pairwise FNC stability from the second-year data was calculated with the weight map[61,62]. Finally, the correlation between actual and predicted cognitive scores was calculated by controlling for the covariates.

Confounding effect of the head motion in children
In this study, we did not exclude those participants with larger head motions because we want to retain more participants to have larger statistical power in the analysis. Head motion during fMRI collections can influence the data quality, which may further impact the estimation of FNC and its stability.

Therefore, we have performed three steps to carefully minimize the impacts of head motion before the estimation of FNC. First, we performed head motion correction in the pre-processing using the FSL toolbox. Rigid body motion correction was performed using the mcflirt tool in FSL. Second, the Neuromark is an ICA-based framework that is capable of extracting networks that are independent of the noise components, such as the head motion. The ICA-based strategy has been widely used for removing motion artefacts in previous studies[63,64]. Third, after extracting the TCs of ICNs, additional post-processing was performed on the TCs to further minimize the influence of head motion. That is, for each TC, we (1) detrended linear, quadratic and cubic trends, (2) removed detected outliers, (3) ran multiple regression of the head motions parameters (three rotations and three translations) and their derivatives, and (4) ran band-pass filtering with a cut-off frequency of 0.01–0.15 Hz. These post-processing procedures have been widely used in previous ICA studies for the removal of head motion effects[7,25,65].

To show the robustness of the association results, we calculated the mean framewise displacement (FD)[66,67] for each scan. The average mean FD for baseline scan 1 is 0.2981 (mean 0.2981, s.d. 0.3697, range ~0.0507–8.7207) and for scan 2 is 0.3526 (mean 0.3526, s.d. 0.4759, range -0.4759–13.7952). For each participant, we averaged mean FD across scans and repeated our analysis by adding this averaged mean FD as one of the fixed effects in the LMM. The overall findings are consistent. Additionally, we also replicated our findings after excluding those participants with large head motions (participants were excluded if one of the scans with head motion >0.3 mean FD). We selected the 0.3 mm threshold because it is mid-range within commonly used thresholds in developmental FC studies[14,68]. Details of these analyses and results are provided in the section 'Replication of the associations by controlling for head motion' in Supplementary Information.

Statistical analysis
The fMRI data were pre-processed using a combination of the FSL v6.0 toolbox and SPM 12 toolbox, under the MATLAB 2020b environment. The multivariate-objective optimization ICA with reference (MOO-ICAR) was used for the estimation of single-scan components in MATLAB 2020b. The significance of identification accuracy was determined by permutation test (1,000 iterations). The significance of associations between FNC stability and health backgrounds was assessed using the LMM in MATLAB 2020b (fitlme function). The multivariate analysis was performed using the PLSR in MATLAB 2020b (plsregress function).

Reporting summary
Further information on research design is available in the Nature Portfolio Reporting Summary linked to this article.

References
1. Park, H. J. & Friston, K. Structural and functional brain networks: from connections to cognition. *Science* **342**, 1238411 (2013).
2. Arbabshirani, M. R., Plis, S., Sui, J. & Calhoun, V. D. Single subject prediction of brain disorders in neuroimaging: promises and pitfalls. *NeuroImage* **145**, 137–165 (2017).
3. Finn, E. S. et al. Functional connectome fingerprinting: identifying individuals using patterns of brain connectivity. *Nat. Neurosci.* **18**, 1664–1671 (2015).
4. Gordon, E. M. & Nelson, S. M. Three types of individual variation in brain networks revealed by single-subject functional connectivity analyses. *Curr. Opin. Behav. Sci.* **40**, 79–86 (2021).
5. Griffa, A., Amico, E., Liégeois, R., Van De Ville, D. & Preti, M. G. Brain structure–function coupling provides signatures for task decoding and individual fingerprinting. *NeuroImage* **250**, 118970 (2022).
6. Horien, C., Shen, X., Scheinost, D. & Constable, R. T. The individual functional connectome is unique and stable over months to years. *NeuroImage* **189**, 676–687 (2019).
7. Allen, E. A. et al. Tracking whole-brain connectivity dynamics in the resting state. *Cereb. Cortex* **24**, 663–676 (2014).
8. Finn, E. S. et al. Can brain state be manipulated to emphasize individual differences in functional connectivity? *NeuroImage* **160**, 140–151 (2017).
9. Giedd, J. N. et al. Brain development during childhood and adolescence: a longitudinal MRI study. *Nat. Neurosci.* **2**, 861–863 (1999).
10. Xia, Y. et al. Tracking the dynamic functional connectivity structure of the human brain across the adult lifespan. *Hum. Brain Mapp.* **40**, 717–728 (2019).
11. Jalbrzikowski, M. et al. Functional connectome fingerprinting accuracy in youths and adults is similar when examined on the same day and 1.5-years apart. *Hum. Brain Mapp.* **41**, 4187–4199 (2020).
12. Demeter, D. V. et al. Functional connectivity fingerprints at rest are similar across youths and adults and vary with genetic similarity. *iScience* **23**, 100801 (2020).
13. Kaufmann, T. et al. Delayed stabilization and individualization in connectome development are related to psychiatric disorders. *Nat. Neurosci.* **20**, 513–515 (2017).
14. Vanderwal, T. et al. Stability and similarity of the pediatric connectome as developmental measures. *NeuroImage* **226**, 117537 (2021).
15. Barch, D. M. et al. Demographic, physical and mental health assessments in the adolescent brain and cognitive development study: rationale and description. *Dev. Cogn. Neurosci.* **32**, 55–66 (2018).

16. Luciana, M. et al. Adolescent neurocognitive development and impacts of substance use: overview of the adolescent brain cognitive development (ABCD) baseline neurocognition battery. *Dev. Cogn. Neurosci.* **32**, 67–79 (2018).

17. Esfahlani, F. Z. et al. High-amplitude cofluctuations in cortical activity drive functional connectivity. *Proc. Natl Acad. Sci. USA* **117**, 28393–28401 (2020).

18. Sporns, O., Faskowitz, J., Teixeira, A. S., Cutts, S. A. & Betzel, R. F. Dynamic expression of brain functional systems disclosed by fine-scale analysis of edge time series. *Netw. Neurosci.* **5**, 405–433 (2021).

19. Cheng, W. et al. Sleep duration, brain structure, and psychiatric and cognitive problems in children. *Mol. Psychiatry* **26**, 3992–4003 (2021).

20. Gorham, L. S., Jernigan, T., Hudziak, J. & Barch, D. M. Involvement in sports, hippocampal volume, and depressive symptoms in children. *Biol. Psychiatry Cogn. Neurosci. Neuroimaging* **4**, 484–492 (2019).

21. Biswal, B. B. et al. Toward discovery science of human brain function. *Proc. Natl Acad. Sci. USA* **107**, 4734–4739 (2010).

22. Váša, F. et al. Conservative and disruptive modes of adolescent change in human brain functional connectivity. *Proc. Natl Acad. Sci. USA* **117**, 3248–3253 (2020).

23. Satterthwaite, T. D. et al. Heterogeneous impact of motion on fundamental patterns of developmental changes in functional connectivity during youth. *NeuroImage* **83**, 45–57 (2013).

24. Marek, S. et al. U. Reproducible brain-wide association studies require thousands of individuals. *Nature* **603**, 654–660 (2022).

25. Fu, Z. et al. Dynamic state with covarying brain activity-connectivity: on the pathophysiology of schizophrenia. *NeuroImage* **224**, 117385 (2021).

26. Laumann, T. O. et al. On the stability of BOLD fMRI correlations. *Cereb. Cortex* **27**, 4719–4732 (2017).

27. Allen, E. A., Damaraju, E., Eichele, T., Wu, L. & Calhoun, V. D. EEG signatures of dynamic functional network connectivity states. *Brain Topogr.* **31**, 101–116 (2018).

28. Wang, H. et al. Functional connectivity predicts individual development of inhibitory control during adolescence. *Cereb. Cortex* **31**, 2686–2700 (2021).

29. Lenroot, R. K. & Giedd, J. N. Sex differences in the adolescent brain. *Brain Cogn.* **72**, 46–55 (2010).

30. Tomescu, M. I. et al. From swing to cane: sex differences of EEG resting-state temporal patterns during maturation and aging. *Dev. Cogn. Neurosci.* **31**, 58–66 (2018).

31. Lenroot, R. K. et al. Sexual dimorphism of brain developmental trajectories during childhood and adolescence. *NeuroImage* **36**, 1065–1073 (2007).

32. Tomescu, M. I. et al. Schizophrenia patients and 22q11.2 deletion syndrome adolescents at risk express the same deviant patterns of resting state EEG microstates: a candidate endophenotype of schizophrenia. *Schizophr. Res. Cogn.* **2**, 159–165 (2015).

33. Hutchison, R. M. et al. Dynamic functional connectivity: promise, issues, and interpretations. *NeuroImage* **80**, 360–378 (2013).

34. Douw, L., Wakeman, D. G., Tanaka, N., Liu, H. & Stufflebeam, S. M. State-dependent variability of dynamic functional connectivity between frontoparietal and default networks relates to cognitive flexibility. *Neuroscience* **339**, 12–21 (2016).

35. Elton, A. & Gao, W. Task-related modulation of functional connectivity variability and its behavioral correlations. *Hum. Brain Mapp.* **36**, 3260–3272 (2015).

36. Hutchison, R. M. & Morton, J. B. Tracking the brain's functional coupling dynamics over development. *J. Neurosci.* **35**, 6849–6859 (2015).

37. Cohen, J. R. The behavioral and cognitive relevance of time-varying, dynamic changes in functional connectivity. *NeuroImage* **180**, 515–525 (2018).

38. Kaiser, R. H. et al. Dynamic resting-state functional connectivity in major depression. *Neuropsychopharmacology* **41**, 1822–1830 (2016).

39. Banich, M. T. et al. Prefrontal regions play a predominant role in imposing an attentional 'set': evidence from fMRI. *Cogn. Brain Res.* **10**, 1–9 (2000).

40. Li, Y. et al. Dynamic functional connectivity reveals abnormal variability and hyper-connected pattern in autism spectrum disorder. *Autism Res.* **13**, 230–243 (2020).

41. Siebenhühner, F., Weiss, S. A., Coppola, R., Weinberger, D. R. & Bassett, D. S. Intra- and inter-frequency brain network structure in health and schizophrenia. *PLoS ONE* **8**, e72351 (2013).

42. Chen, G. et al. Shared and specific patterns of dynamic functional connectivity variability of striato-cortical circuitry in unmedicated bipolar and major depressive disorders. *Psychol. Med.* **52**, 747–756 (2022).

43. Paul, S. E. et al. Associations between prenatal cannabis exposure and childhood outcomes: results from the ABCD study. *JAMA Psychiatry* **78**, 64–76 (2021).

44. Thompson, B. Effect sizes, confidence intervals, and confidence intervals for effect sizes. *Psychol. Sch.* **44**, 423–432 (2007).

45. Schäfer, T. & Schwarz, M. A. The meaningfulness of effect sizes in psychological research: differences between sub-disciplines and the impact of potential biases. *Front. Psychol.* **10**, 813 (2019).

46. Götz, F. M., Gosling, S. D. & Rentfrow, P. J. Small effects: the indispensable foundation for a cumulative psychological science. *Perspect. Psychol. Sci.* **17**, 205–215 (2022).

47. Tiego, J. et al. Precision behavioral phenotyping as a strategy for uncovering the biological correlates of psychopathology. *Nat. Ment. Heal.* **1**, 304–315 (2023).

48. van der Sluis, S., Verhage, M., Posthuma, D. & Dolan, C. V. Phenotypic complexity, measurement bias, and poor phenotypic resolution contribute to the missing heritability problem in genetic association studies. *PLoS ONE* **5**, e13929 (2010).

49. Chang, C. & Glover, G. H. Time-frequency dynamics of resting-state brain connectivity measured with fMRI. *NeuroImage* **50**, 81–98 (2010).

50. Fu, Z., Abbott, C. C., Sui, J. & Calhoun, V. D. Predictive signature of static and dynamic functional connectivity for ECT clinical outcomes. *Front. Pharmacol.* **14**, 1102413 (2023).

51. Du, Y. et al. NeuroMark: an automated and adaptive ICA based pipeline to identify reproducible fMRI markers of brain disorders. *Neuroimage Clin.* **28**, 102375 (2020).

52. Fu, Z. et al. Dynamic functional network connectivity associated with post-traumatic stress symptoms in COVID-19 survivors. *Neurobiol. Stress* **15**, 100377 (2021).

53. Tu, Y. et al. Distinct thalamocortical network dynamics are associated with the pathophysiology of chronic low back pain. *Nat. Commun.* **11**, 4347 (2020).

54. Li, K. et al. The influence of cerebral small vessel disease on static and dynamic functional network connectivity in subjects along Alzheimer's disease continuum. *Brain Connect.* **11**, 189–200 (2021).

55. Fu, Z. et al. Whole-brain functional connectivity dynamics associated with electroconvulsive therapy treatment response. *Biol. Psychiatry Cogn. Neurosci. Neuroimaging* **7**, 312–322 (2022).

56. Fu, Z. et al. Dynamic functional network reconfiguration underlying the pathophysiology of schizophrenia and autism spectrum disorder. *Hum. Brain Mapp.* **42**, 80–94 (2021).

57. Smith, S. M. et al. Correspondence of the brain's functional architecture during activation and rest. *Proc. Natl Acad. Sci. USA* **106**, 13040–13045 (2009).

58. Du, Y. & Fan, Y. Group information guided ICA for fMRI data analysis. *NeuroImage* **69**, 157–197 (2013).

59. Dick, A. S. et al. No evidence for a bilingual executive function advantage in the nationally representative ABCD study. *Nat. Hum. Behav.* **3**, 692–701 (2019).

60. Benjamini, Y. & Hochberg, Y. Controlling the false discovery rate: a practical and powerful approach to multiple testing. *J. R. Stat. Soc. Ser. B* **57**, 289–300 (1995).

61. Jiang, R. et al. A neuroimaging signature of cognitive aging from whole-brain functional connectivity. *Adv. Sci.* **9**, 2201621 (2022).

62. Kucyi, A. et al. Prediction of stimulus-independent and task-unrelated thought from functional brain networks. *Nat. Commun.* **12**, 1793 (2021).

63. Pruim, R. H. R. et al. ICA-AROMA: a robust ICA-based strategy for removing motion artifacts from fMRI data. *NeuroImage* **112**, 267–277 (2015).

64. Parkes, L., Fulcher, B., Yücel, M. & Fornito, A. An evaluation of the efficacy, reliability, and sensitivity of motion correction strategies for resting-state functional MRI. *NeuroImage* **171**, 415–436 (2018).

65. Tu, Y. et al. Distinct thalamocortical network dynamics are associated with the pathophysiology of chronic low back pain. *Nat. Commun.* **11**, 3948 (2020).

66. Patel, A. X. et al. A wavelet method for modeling and despiking motion artifacts from resting-state fMRI time series. *NeuroImage* **95**, 287–304 (2014).

67. Power, J. D., Barnes, K. A., Snyder, A. Z., Schlaggar, B. L. & Petersen, S. E. Spurious but systematic correlations in functional connectivity MRI networks arise from subject motion. *NeuroImage* **59**, 2142–2154 (2012).

68. Dosenbach, N. U. F. et al. Real-time motion analytics during brain MRI improve data quality and reduce costs. *NeuroImage* **161**, 80–93 (2017).

Author contributions

Z.F. and V.D.C. designed the study; Z.F. performed the data analysis; Z.F., J.L., J.S. and V.D.C. wrote the paper. M.S.S. helped with data pre-processing. All authors contributed to the results interpretation and discussion.

Competing interests

The authors declare no competing interests.

Additional information

Supplementary information The online version contains supplementary material available at https://doi.org/10.1038/s44220-023-00151-8.

Correspondence and requests for materials should be addressed to Zening Fu.

Peer review information *Nature Mental Health* thanks Seok-Jun Hong, Doug Schultz and the other, anonymous, reviewer(s) for their contribution to the peer review of this work.

Reprints and permissions information is available at www.nature.com/reprints.

Publisher's note Springer Nature remains neutral with regard to jurisdictional claims in published maps and institutional affiliations.

Corresponding author(s):   Zening Fu

Last updated by author(s):   Sep 22, 2023

Reporting Summary

Nature Portfolio wishes to improve the reproducibility of the work that we publish. This form provides structure for consistency and transparency in reporting. For further information on Nature Portfolio policies, see our Editorial Policies and the Editorial Policy Checklist.

Statistics

For all statistical analyses, confirm that the following items are present in the figure legend, table legend, main text, or Methods section.

n/a	Confirmed	
☐	☒	The exact sample size (n) for each experimental group/condition, given as a discrete number and unit of measurement
☐	☒	A statement on whether measurements were taken from distinct samples or whether the same sample was measured repeatedly
☐	☒	The statistical test(s) used AND whether they are one- or two-sided *Only common tests should be described solely by name; describe more complex techniques in the Methods section.*
☐	☒	A description of all covariates tested
☐	☒	A description of any assumptions or corrections, such as tests of normality and adjustment for multiple comparisons
☐	☒	A full description of the statistical parameters including central tendency (e.g. means) or other basic estimates (e.g. regression coefficient) AND variation (e.g. standard deviation) or associated estimates of uncertainty (e.g. confidence intervals)
☐	☒	For null hypothesis testing, the test statistic (e.g. F, t, r) with confidence intervals, effect sizes, degrees of freedom and P value noted *Give P values as exact values whenever suitable.*
☒	☐	For Bayesian analysis, information on the choice of priors and Markov chain Monte Carlo settings
☒	☐	For hierarchical and complex designs, identification of the appropriate level for tests and full reporting of outcomes
☐	☒	Estimates of effect sizes (e.g. Cohen's d, Pearson's r), indicating how they were calculated

Our web collection on statistics for biologists contains articles on many of the points above.

Software and code

Policy information about availability of computer code

Data collection	No software was used in data collection.
Data analysis	MATLAB 2020b can be download at https://www.mathworks.com. The FSL 6.0.2 toolbox can be download at https://fsl.fmrib.ox.ac.uk/fsl/fslwiki. The SPM 12 toolbox can be downloaded at https://www.fil.ion.ucl.ac.uk/spm/. The codes of the Neuromark framework and the Neuromark template have been released and integrated into the group ICA Toolbox (GIFT 4.0c, https://trendscenter.org/software/gift/). which can be downloaded and used directly by users worldwide. Other MATLAB codes of this study can be obtained from the corresponding author.

For manuscripts utilizing custom algorithms or software that are central to the research but not yet described in published literature, software must be made available to editors and reviewers. We strongly encourage code deposition in a community repository (e.g. GitHub). See the Nature Portfolio guidelines for submitting code & software for further information.

Data

The ABCD data used in the present study can be accessed upon application from NDA (https://nda.nih.gov/) with the approval of the ABCD consortium. The digital object identifier (DOI) of the ABCD data is 10.15154/1520591.

Human research participants

Policy information about studies involving human research participants and Sex and Gender in Research.

Reporting on sex and gender	Our findings apply to both sexes. In this study, we used the sex of the subject at birth, which is the assignment as male or female based on the biological attribute. Birth sex is measured by the PhenX toolkit. We focused on the general patterns in children aged 9-11 years and also separated our analysis for each sex respectively. When using all samples, we controlled for sex in the linear mixed-effect model as one of the fixed effects to remove the influence of sex on the statistical analysis. Our discovery sample includes 4365 females and 4706 males (in total 9071 subjects). Content has been obtained for sharing of sex information by the ABCD study.
Population characteristics	Baseline: Age (month): 119.06 ± 7.52 Gender (F/M): 4365/4706 Height (inch): 55.28 ± 3.35 Weight (lbs): 82.97 ± 23.52 Race (W/B/H/A/O): 4771/1325/1863/181/929 Second-year: Age (month): 142.86 ± 7.51 Gender (F/M): 1333/1585 Height (inch): 60.04 ± 3.53 Weight (lbs): 107.57 ± 31.99 Race (W/B/H/A/O): 1631/317/629/57/284
Recruitment	Participants were recruited from the ABCD, which is a recently-initiated national consortium that includes 21 data collection sites throughout the United States. The goal of ABCD is to follow a large number of children, recruited at ages 9–10, for a ten-year span through adolescence and into young adulthood in order to relate neurodevelopment to environmental exposures such as substance use as it emerges within the sample. Our study used the neuroimaging data from the amendment ABCD Fix Release 2.0.1, made publicly available in July 2019. Data Release 2.01 from the ABCD consortium contains over 11,000 children aged 9–11 years with a diverse range of geographic, socioeconomic, ethnic, and health backgrounds.
Ethics oversight	The parent's full written informed consent and the child's assent were obtained under protocols approved by the Institutional Review Board (IRB). The University of California, San Diego provided centralized IRB approval and each participating site received local IRB approval.

Note that full information on the approval of the study protocol must also be provided in the manuscript.

Field-specific reporting

Please select the one below that is the best fit for your research. If you are not sure, read the appropriate sections before making your selection.

☒ Life sciences   ☐ Behavioural & social sciences   ☐ Ecological, evolutionary & environmental sciences

For a reference copy of the document with all sections, see nature.com/documents/nr-reporting-summary-flat.pdf

Life sciences study design

All studies must disclose on these points even when the disclosure is negative.

Sample size	We performed QC on the preprocessed fMRI data via the Neuromark framework. Participants who did not show good normalization of their fMRI images to the MNI standard space were excluded from further analysis. Specifically, we compared individual masks with the group mask and retained those subjects with a high similarity between the individual masks and the group mask. This method can ensure we have a high-quality mask and fMRI data for all individuals and has been shown to work well in our previous studies. In this study, we only included subjects with enough good resting-state scans for further analysis. For the within-session analysis, there are

Data exclusions	9071 subjects with four good scans from the baseline session and 2918 subjects with four good scans from the second-year session. For the cross-session analyses, there are 2290 subjects with four good scans from the baseline session and also four good scans from the second-year session. We also provided a flowchart in the supplementary information to describe how to include subjects and scans in our study. We performed data quality control on the preprocessed fMRI data via the Neuromark framework. Participants who did not show good normalization of their fMRI images to the MNI standard space were excluded from further analysis. Specifically, we compared individual masks with the group mask and retained those subjects with a high similarity between the individual masks and the group mask. First, based on the first fMRI time volume, we calculated the individual mask for each subject by setting voxels to 1 if they are greater than 90% of the whole brain mean. Next, we computed a group mask by setting voxels to 1 if they have more than 90% of the subjects with 1 for individual masks. For each subject, we then calculated the spatial correlations between the group mask and the individual mask. The spatial correlations were calculated using voxels within the top 10 slices of the mask, within the bottom 10 slices of the mask, and of the whole mask, resulting in three correlations for each subject. If a subject has a top-10-slices correlation larger than 0.75, a bottom-10-slices correlation larger than 0.55, and a whole-brain correlation larger than 0.8, we include this subject for further analysis. This method can ensure we have a high-quality mask and fMRI data for all individuals and has been shown to work well in our previous studies. As we would like to examine the test-retest reliability of our analysis, we selected subjects with at least four good scans within either the baseline session or the second-year session.
Replication	The individual identification was replicated using four resting-state scans within the baseline session (N = 9071) and further replicated using four resting-state scans from the second-year session (N = 2918). The individual identification was also replicated between longitudinal scans with a two-year interval (N = 2290). The brain-behavior association results were replicated by controlling for the head motions and by using subjects with small head motions (N = 5549). The brain-behavior association results were also replicated across data from different scanners. The brain-behavior association results were further replicated using the second-year data.
Randomization	There is only one group in our analysis. Age, gender, race, height, and weight were considered confounding effects and were modeled as fixed effects. The family structures and sites were modeled as random effects.
Blinding	Blinding is not possible because there is only one group in our analysis. We controlled the covariates in the statistical analysis and replicated the results across multiple scans from longitudinal sessions.

Reporting for specific materials, systems and methods

We require information from authors about some types of materials, experimental systems and methods used in many studies. Here, indicate whether each material, system or method listed is relevant to your study. If you are not sure if a list item applies to your research, read the appropriate section before selecting a response.

Materials & experimental systems

n/a	Involved in the study
☒	☐ Antibodies
☒	☐ Eukaryotic cell lines
☒	☐ Palaeontology and archaeology
☒	☐ Animals and other organisms
☒	☐ Clinical data
☒	☐ Dual use research of concern

Methods

n/a	Involved in the study
☒	☐ ChIP-seq
☒	☐ Flow cytometry
☐	☒ MRI-based neuroimaging

Magnetic resonance imaging

Experimental design

Design type	Resting state fMRI
Design specifications	NO task fMRI were included in our current study.
Behavioral performance measures	NO task fMRI were included in our current study.

Acquisition

Imaging type(s)	functional
Field strength	3T
Sequence & imaging parameters	High spatial and temporal resolution multiband echo-planar imaging (EPI) resting-state fMRI data with fast integrated distortion correction are acquired using three 3T scanner platforms: Siemens Prisma, General Electric (GE) 750, and Phillips. Resting-state fMRI parameters are similar across platforms: a standard multiband EPI sequence, repetition time (TR)/echo time (TE) = 800/30 ms, voxel spacing size = 2.4 × 2.4 × 2.4 mm, slice number = 60, flip angle (FA) = 52°, field of view (FOV) = 216 × 216 mm, multiband acceleration = 6, and a total acquisition time is around 5 min.
Area of acquisition	53 intrinsic connectivity networks (ICNs) were extracted by the Neuromark framework, with activation peaks falling on the majority of cortical and subcortical gray matter areas across the whole brain. The ICNs were assigned to seven different functional domains according to their anatomical locations and functional information, including subcortical (SC), auditory (AUD), visual (VS), sensorimotor (SM), cognitive-control (CC), default-mode (DM), and cerebellar (CB) domains. The Neuromark framework leverages an adaptive ICA technique that automates the estimation of reproducible functional brain markers across subjects, datasets, and studies. A set of template components were used to extract comparable components across subjects, scans, and sessions from the ABCD data. The network templates were constructed using two independent resting-state fMRI datasets with large samples of healthy subjects (1828 healthy subjects in total): the human connectome project (HCP) and the genomics superstruct project (GSP).

Diffusion MRI ☐ Used ☒ Not used

Preprocessing

Preprocessing software	FSL6.0.2 and SPM12
Normalization	Non-linear
Normalization template	EPI template
Noise and artifact removal	We preprocessed the raw fMRI data using a combination of the FMRIB Software Library (FSL) v6.0 toolbox and Statistical Parametric Mapping (SPM) 12 toolbox, under the MATLAB 2019b environment. Rigid body motion correction was performed using the mcflirt tool in FSL before the distortion correction. The ABCD fMRI field map data were collected with the phase-reversed blips, producing pairs of images with distortion occurring in opposite directions. Volumes acquired with phase encoding in the anterior-posterior (AP) direction and volumes with phase encoding in the posterior-anterior (PA) direction were used with the FSL tool topup to estimate the susceptibility-induced off-resonance field. The output field map coefficients were used to correct the distortion in the fMRI volume using the FSL tool applytopup. After distortion correction, we discarded 10 initial scans with large signal changes to allow the tissue to reach a steady-state of radiofrequency excitation. Next, the fMRI data were warped into the standard Montreal Neurological Institute (MNI) space based on the echo-planar imaging (EPI) template, resampling to 3 × 3 ×3 mm3 isotropic voxels using the normalization tool in SPM. The resliced fMRI images were subsequently smoothed using a Gaussian kernel with a full width at half maximum (FWHM) = 6 mm. After the preprocessing, we adopted the Neuromark framework, which extracted meaningful components independent of the noise components, such as the head motion. The 53 components selected for the FNC analysis are important gray matter networks, which are orthogonal to the noise components. Finally, we performed postprocessing on the time courses of the components, including detrending linear, quadratic, and cubic trends, removing outliers, regressing out head motions and their derivatives, and filtering, which further minimized the head motion impacts on the FNC estimation.
Volume censoring	We performed quality control on the preprocessed fMRI data via the Neuromark framework. Participants who did not show good normalization of their fMRI images to the MNI standard space were excluded from further analysis. Specifically, we compared individual masks with the group mask and retained those subjects with a high similarity between the individual masks and the group mask. First, based on the first fMRI time volume, we calculated the individual mask for each subject by setting voxels to 1 if they are greater than 90% of the whole brain mean. Next, we computed a group mask by setting voxels to 1 if they have more than 90% of the subjects with 1 for individual masks. For each subject, we then calculated the spatial correlations between the group mask and the individual mask. The spatial correlations were calculated using voxels within the top 10 slices of the mask, within the bottom 10 slices of the mask, and of the whole mask, resulting in three correlations for each subject. If a subject has a top-10-slices correlation larger than 0.75, a bottom-10-slices correlation larger than 0.55, and a whole-brain correlation larger than 0.8, we include this subject for further analysis. This method can ensure we have a high-quality mask and fMRI data for all individuals and has been shown to work well in our previous studies.

Statistical modeling & inference

Model type and settings	Classification, univariate, multivariate and predictive
Effect(s) tested	No task fMRI were included in this study.

Specify type of analysis: ☐ Whole brain ☐ ROI-based ☒ Both

Anatomical location(s)	To capture reliable intrinsic connectivity networks (ICNs) and their corresponding time-courses (TCs) for each subject and each scan, a robust ICA-based framework called Neuromark was applied to the ABCD data. Unlike atlas-based methods that typically assume fixed brain regions across subjects, the Neuromark can identify brain networks comparable across subjects while adapting single-subject variability with the networks. The effectiveness of Neuromark has been demonstrated in previous work, with a wide range of brain markers and abnormalities identified in different populations.

Statistic type for inference
(See Eklund et al. 2016)

cluster-wise, we focused on the functional connectivity between brain regions across the whole brain.

Correction

FDR

Models & analysis

n/a	Involved in the study
☐ ☒	Functional and/or effective connectivity
☒ ☐	Graph analysis
☐ ☒	Multivariate modeling or predictive analysis

Functional and/or effective connectivity

Pearson correlation

Multivariate modeling and predictive analysis

The cross-scan FNC stability was measured by the intra-subject similarity between the FNC of scan 1 and the mean FNC across scans 2~4. To show the test-retest reliability of the associations, we also replicated the results using different FNC stability measures and using the second-year data.

A linear mixed-effect model (LMM) was adopted to investigate the associations between intra-subject cross-scan FNC stability and behavioral assessments. The LMM was also used to examine the associations between the children's FNC stability and their parents' conditions and neighborhood safety. The ABCD data contain related data at sites and within families due to twins and siblings. The LMM can model families nested within the site to take account of this effect. It has been successfully applied in previous ABCD studies and identified meaningful brain-wide associations with a wide range of individual behaviors. In this work, cross-scan FNC stability was modeled as the dependent variable, while each score/behavior was modeled as a fixed effect. Age, gender, race, height, and weight were considered confounding effects and were modeled as other fixed effects. The family structures and sites were modeled as random effects. The correlation r-value, t-statistic, and effect size Cohen's d were obtained for each association analysis to reflect the relationship between FNC stability and a behavioral score. The results are corrected by false discovery rate (FDR) correction.

In addition, we performed analyses using a multivariate predictive technique, namely partial least squares regression (PLSR). PLSR is one of the most popular prediction models in neuroimaging that can establish reliable brain-behavior relationships. It works by projecting high-dimensional features into a small set of components without using prior feature selection. Here, we chose the domain-based FNC stability as the imaging feature because it has relatively larger dimensions.

Considering that multivariate methods will significantly benefit from high-dimensional features, we also developed a method to evaluate cross-scan FNC stability for each pair of FNC, which can provide high-dimensional FNC stability features for building the prediction model. Via this method, we extracted 1378 FNC stability features for each subject, which were used as the input of the PLSR model. PLSR projected these high-dimensional features into a small set of components without prior feature selection.

We selected the composite cognitive scores as the target measures, which show the largest associations with cross-scan FNC stability in the univariate analyses. We utilized 10-fold nested cross-validation with 1000 random replications to avoid circularity bias. In each cross-validation, an optimal predictive model was established using the training data to capture the relationships between cross-scan FNC stability and the target measure to be predicted. The predictive model was then applied to the testing data, generating a predictive score for each subject in the testing data. By iteratively designating each fold of data as a testing set once, we can obtain the predictive scores for all subjects. Model performance was quantified as the correlation r between actual and predicted scores, averaged across 1000 repetitions. The same covariates as in the main text were controlled in cross-validation to show that our predictive models are robust to these confounds. To examine the significance of the association, we performed a non-parametric permutation test by shuffling the correspondence between imaging features and the target measure 1000 times and then repeating the nested cross-validated predictive analysis, generating a null distribution of 1000 correlations. The significance of the correlation was estimated by calculating the frequency with which the permutation-derived correlations exceeded the actual correlation.